Evaluation of Mechanical Properties and microstructures of Direct-Quenched- and direct quenched and tempered Microalloyed Ultrahigh-Strength Steels

Jaakko Hannula*, Antti Kaijalainen, David A. Porter, Mahesh C. Somani, Jukka Kömi

Jaakko Hannula, Antti Kaijalainen, David A. Porter, Mahesh C. Somani, Jukka Kömi
University of Oulu, Materials and Mechanical Engineering
Faculty of Technology, P.O. Box 4200
90014 Oulu
Finland
E-mail: Jaakko.hannula@oulu.fi

This paper reveals the effects of molybdenum and niobium on the microstructures and mechanical properties of laboratory rolled and direct-quenched and direct-quenched and tempered steels. The microstructures are martensitic with yield strength of 766 – 1119 MPa in direct quenched condition, and 632 – 1011 MPa in direct quenched and tempered condition. Mo and Nb additions lead to a fine martensitic microstructure that impart a good combination of strength and toughness. Steel with 0.5 wt.% molybdenum has a high yield strength of 1119 MPa combined with low 28J transition temperature of −95 °C in direct quenched condition. Molybdenum and niobium increase the strength significantly during tempering due to enhanced solute drag and precipitation hardening. Addition of 0.25 wt.% molybdenum increases yield strength from 632 MPa to 813 MPa after tempering. However, the combination of niobium and molybdenum results in even greater increase in yield strength during tempering compared to non-alloyed version producing almost 400 MPa increase in yield strength. Transmission electron microscopy reveals that only niobium forms stable precipitates during tempering, indicating that molybdenum largely remains in solution. X-ray diffraction analysis elucidates that molybdenum and molybdenum-niobium alloying prevent annihilation of dislocations leading to the presence of high densities of dislocations after tempering.

1. Introduction

Energy efficiency and environmental issues have become a critical concerns in recent years and the possibility of making lighter and more energy-efficient structures with ultrahigh-strength steels has become more important. To achieve suitable properties for ultrahigh-strength steels, thermomechanically controlled processing (TMCP) combined with direct quenching (DQ) can be considered as novel and more effective processing route in order to achieve properties, such as high-strength and good toughness, for demanding applications. In addition, subsequent tempering following hot rolling and direct quenching can be carried out to produce good combination of strength, ductility, impact toughness, and low ductile-to-brittle transition temperature.[1] Compared to conventional reheating and quenching process route, as a perspective of energy efficient, direct quenching produces significant benefits due to lack of energy-intensive reheating process step.

Re-heating and quenching prior to tempering (RQT) has been a well-established process to produce high-strength steels.[2] Mo alloying has been conventionally applied in ultrahigh-strength (UHSS) RQT steels, and it has been found to increase the hardenability and improve the tempering resistance.[3] Also niobium alloying has been used in high-strength steels for hindering grain growth during slab reheating, controlling grain size during hot rolling, and increasing strength during tempering by precipitation strengthening.[4–6] Especially in case of tempered steels, the precipitation strengthening has a key role. The roles of niobium and molybdenum individually have been widely studied, but recently several studies have shown that the combination of Nb-Mo alloying can have even greater influence on precipitation kinetics and further on tempering resistance.[7,8]For example, Wang et al. [7]discovered that addition of Mo reduced the precipitation size in Mo-Nb-V steel, when tempering at 650 °C, which was caused by the segregation of Mo at the outer layer of carbides inhibiting the diffusion of Nb from the matrix into the carbides.

Also dislocation density has a major role in preserving high strength after tempering. Previous studies have shown that it is possible to reduce the annihilation of dislocations during tempering by microalloying.[9,10]

This paper is a continuation end extension of previous work by the authors, which focused on the effect of molybdenum and niobium on direct quenched steels.[5] In this paper, contrary to already published work, the focus is related to the effect of tempering procedure using the same steel compositions. However, part of the results from previous published work [5], have been used in this study to compare the properties of the investigated steels both in direct quenched- and direct quenched and tempered conditions.

2. Experimental

2.1. Materials and heat treatment

The investigated materials were low-carbon (~0.16 wt.%) steels with manganese, chromium, nickel and boron alloying as seen in Tab. 1. The compositions studied covered three molybdenum levels, i.e. 0, 0.25 and 0.5 wt.% Mo. A fourth composition bearing 0.25 wt.% Mo was also alloyed with 0.04 wt.% Nb. Each steel was coded based on the contents of Mo and Nb. The chosen compositions (Tab.1) were vacuum-cast into approximately 70 kg slabs at the Tornio Research Centre of Outokumpu Oyj in Finland. 180 x 80 x 55 mm pieces of the castings were soaked at 1100 °C for 2 hours and thermomechanically rolled to approximately 11 mm thick plates according to the rolling schedule given in Tab. 2. The temperature of the samples during rolling and direct quenching was monitored and controlled by thermocouples placed in the middle of the rolled samples in the edges of the samples to the mid-width at mid-length. A finish rolling temperature (FRT) of 900 °C (accuracy ± 20 °C) was used prior to quenching in a water bath with a cooling rate in range of 40-50 °C/s. Tempering experiments were carried out for the selected hot rolled samples in a furnace maintained at a

temperature of 600 °C with ~30 minutes holding at the peak temperature followed by air cooling to room temperature.

Table. 1 Chemical compositions of the investigated steels (in wt.%)

Steel	C	Si	Mn	Cr	Ni	Mo	Nb	Al	B	N
0Mo	0.16	0.2	1.0	0.5	0.5	-	-	0.03	0.0015	0.0050
0.25Mo	0.16	0.2	1.1	0.5	0.5	0.25	-	0.03	0.0015	0.0043
0.5Mo	0.16	0.2	1.1	0.5	0.5	0.5	-	0.03	0.0015	0.0051
0.25Mo-Nb	0.16	0.2	1.1	0.5	0.5	0.25	0.04	0.03	0.0015	0.0047

Table. 2 Pass schedule of hot rolling trials.

Pass	Thickness [mm]	Temperature [°C]	Reduction per pass [%]	Total reduction [%]	Reduction after pass 3 [%]
-	52	1100			
1	42	1100	19	19	
2	33	1080	21	37	
3	26	1060	21	50	
4	20	1030	23	62	23
5	15	960	25	71	42
6	11.2	900	25	78	57

2.2. Mechanical properties

Tensile and Charpy-V impact tests were performed in longitudinal direction to evaluate the strength and low temperature toughness properties, respectively. Three tensile tests were performed using round bar specimens with a diameter of 6 mm according to the standard ISO 6892-1:2016.[11] Charpy-V impact tests were performed at various temperatures (2 specimen/temperature) according to the standard ISO 10 148-1:2016[12] to derive Charpy V-transition curves using 10 x 10 x 55 mm3 standard specimens.

2.3. Microstructural characterization

Microstructural characterization was carried out using laser scanning confocal optical microscopy (LSCM), field-emission scanning electron microscopy (Zeiss Zigma) combined with electron backscatter diffraction (EDAX-OIM) (FESEM-EBSD) and transmission electron microscopy (JEOL JEM-2200FS) (TEM). The linear intercept method applied to

laser scanning confocal microscopy (LSCM) images from specimens etched in saturated picral with soap solution [13] was used to determine the prior austenite grain sizes in three principal directions: the rolling direction (RD), transverse to the rolling direction (TD) and in the plate normal direction (ND) at the quarter-thickness of the specimen. Based on the measurements, the aspect ratio (r), total reduction below the recrystallization temperature (Rtot), the surface area per unit volume (Sv) and average grain size (d) were determined using the equations shown in Table 3.[14]

EDAX-OIM acquisition and analysis software were used to EBSD measurements and data analyses. The FESEM required for the EBSD measurements was operated at accelerating voltage of 15 kV using a step size of 0.15 micrometers. Lath and effective grain sizes were defined as equivalent circle diameter (ECD) values with low-angle (>2.5°) and high-angle boundary misorientation (15–63°), respectively.

X-Ray diffraction (XRD) analyses were carried out using Rigaku SmartLab 9 kW X-ray diffractometer with Cu Kα radiation. Data analysis was executed using PDXL2 analysis software to determine the lattice parameters, microstrains and crystallite sizes of the investigated steels. The samples for XRD analysis were ground to quarter thickness from the surface of the sample prior to polishing with colloidal silica suspension. Furthermore, dislocation densities were calculated using the Williamson-Hall method (Equation 1):[15,16]

$$\rho = \sqrt{\rho_s \rho_p} \qquad (1)$$

where ρs is dislocation density calculated from strain broadening and ρp is dislocation density calculated from particle i.e. crystallite size, (Equations 2 & 3). In addition, according to Williamson et al.:[15,16]

$$\rho_s = \frac{k \varepsilon^2}{F b^2} \qquad (2)$$

and

$$\rho_p = \frac{3n}{D^2} \tag{3}$$

where ε is microstrain, b is the burgers vector, F is an interaction factor (assumed as 1), factor k is assumed as 14.4 for body-centered cubic metals, and D corresponds to crystallite size. In the equation 3, n stands for dislocations per block face, (assumed as 1). This assumption is based on Williamson et al. [16], where it is stated that the metal is broken up into blocks and the dislocations are lying in the boundaries between the blocks, which gives the assumed value (n as 1) leading to the minimum dislocation density.

Table. 3 Austenite grain structure parameters [14].

Parameter	Equation
R_{tot}	$1- \sqrt{(1/ d_{RD}/d_{ND})}$ tai $1- \sqrt{(d_{ND}/d_{RD})}$
S_v	$0.429 \times (1/d_{RD}) + 0.571 \times (1/d_{TD}) + (1/d_{ND})$
d	$(d_{RD} \times d_{TD} \times d_{ND})^{\frac{1}{3}}$

3. Results and discussion

3.1. Prior austenite grain structure after hot rolling

Austenite grain structure after hot rolling (FRT 900 °C) and direct quenching was examined to see the effect of Mo and Nb alloying on the recrystallization and pancaking of austenite structure. The differences in prior austenite grain structures and the influence of Mo and Nb in increasing the degree of austenite pancaking are evident from Fig. 1. Some small grains can be seen in 0.25Mo steel nucleated at grain boundaries implying that partial recrystallization might occur with a FRT of 900 °C. Tab. 4 shows the measured austenite grain sizes, calculated S_v values and corresponding R_{tot} values after hot rolling. Generally, the S_v values and reduction percentages below the recrystallization temperature were higher when a combination of Mo and Nb microalloying (0.25Mo-Nb steel) was used. Mo alloying did retard the recrystallization process without the presence of Nb, however the combination of Nb and Mo had the greatest effect on delaying the recrystallization process (see Tab. 4).

Comparing the values of R_{tot} in Tab. 2, the reductions after pass 3 indicates that for the present rolling conditions, recrystallization ceases at 1030 °C or possibly higher in the case of the 0.25Mo-Nb composition. Without Mo and Nb alloying, austenite grain structure was almost equiaxed (Fig. 2a). Prior austenite grain size measurements after hot rolling confirmed that Mo itself affects the recrystallization kinetics, as expected, and increases the no-recrystallization temperature (T_{NR})leading to a higher degree of deformed austenite structure. However, no clear differences in austenite grain structure can be seen by comparing the results of 0.25Mo and 0.5Mo steels. Earlier studies have shown that Mo affects the dynamic recrystallization (DRX) kinetics by increasing the activation energy through strong solute drag leading to the retardation of DRX .[17,18]Similarly, Pereda et al. [17] have shown that there is no difference in DRX behaviour between low carbon steels with 0.15 and 0.3 wt.% of Mo, and based on our results, also 0.5 wt.% Mo does not contribute to any additional effect on DRX behaviour. This indicates that the saturation point for effectiveness of Mo on delaying DRX is less than 0.15 wt.% of Mo. Also, in the case of 0Mo steel (Fig. 1a) small grains can be seen at prior austenite grain boundaries, which are not present in the case of other steels. These grains refer to minor ferrite formation during subsequent cooling after hot rolling.
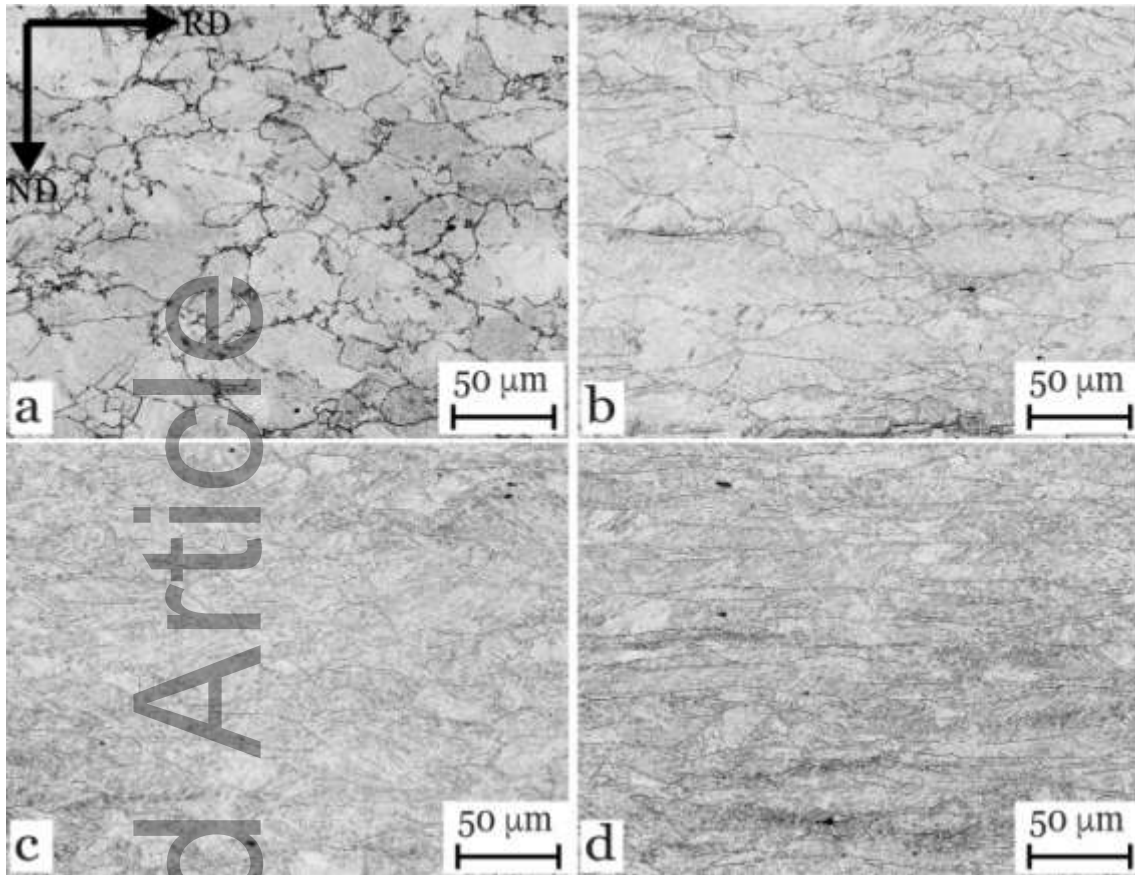
Figure 1. Prior austenite grain boundaries of the investigated steels with FRT 900°C, a) 0Mo, b) 0.25Mo, c) 0.5Mo and d) 0.25Mo-Nb.

Table. 4 Mean prior austenite grain sizes in three principal directions and corresponding d, S_v and R_{tot} at the quarter-thickness of the specimen.

FRT	Steel	d_{RD} [μm]	d_{ND} [μm]	d_{TD} [μm]	d [μm]	S_v [mm²/mm³]	R_{tot} [%]
	0Mo	19.2±2.4	14.9± 1.7	19.5± 2.1	17.7± 1.2	119	12.0
900 °C	0.25Mo	19.2± 2.2	8.4± 1	15.9± 1.9	13.7± 0.9	177	33.8
	0.5Mo	16.1±1.8	7.4± 0.6	12.2± 1.2	11.3± 0.6	210	32.4
	0.25Mo-Nb	23.5± 2.2	5.8± 0.5	14.5± 1.6	12.6± 0.7	229	50.2

3.2. Transformed microstructure

After hot rolling, transformed microstructures were evaluated using field emission scanning electron microscopy (FESEM) and transmission electron microscopy (TEM). Fig. 2 shows typical microstructures of the investigated steels in the as-quenched condition at the quarter depth position of the plate. Generally, the microstructures consisted of fine packets and blocks of martensitic laths with randomized orientation. Also very fine carbides within the martensite laths were found in some parts of the microstructures, which indicate that auto-tempering of

martensite occurred partially. Based on microstructural characterizations, hot rolling using finish rolling temperature of 900 °C and direct quenching produced mainly martensitic microstructures in all cases regardless of the increase in Mo or Mo-Nb alloying (Fig. 2). However, in case of 0Mo steel (Fig. 2a) some grain boundary ferrite was found in some parts of the investigated sample. Indication of ferrite formation was already seen in investigation of prior austenite grain boundaries (Fig. 1a). Already the addition of 0.25 wt.% of molybdenum prevented the ferrite formation, as seen from Fig. 2b.
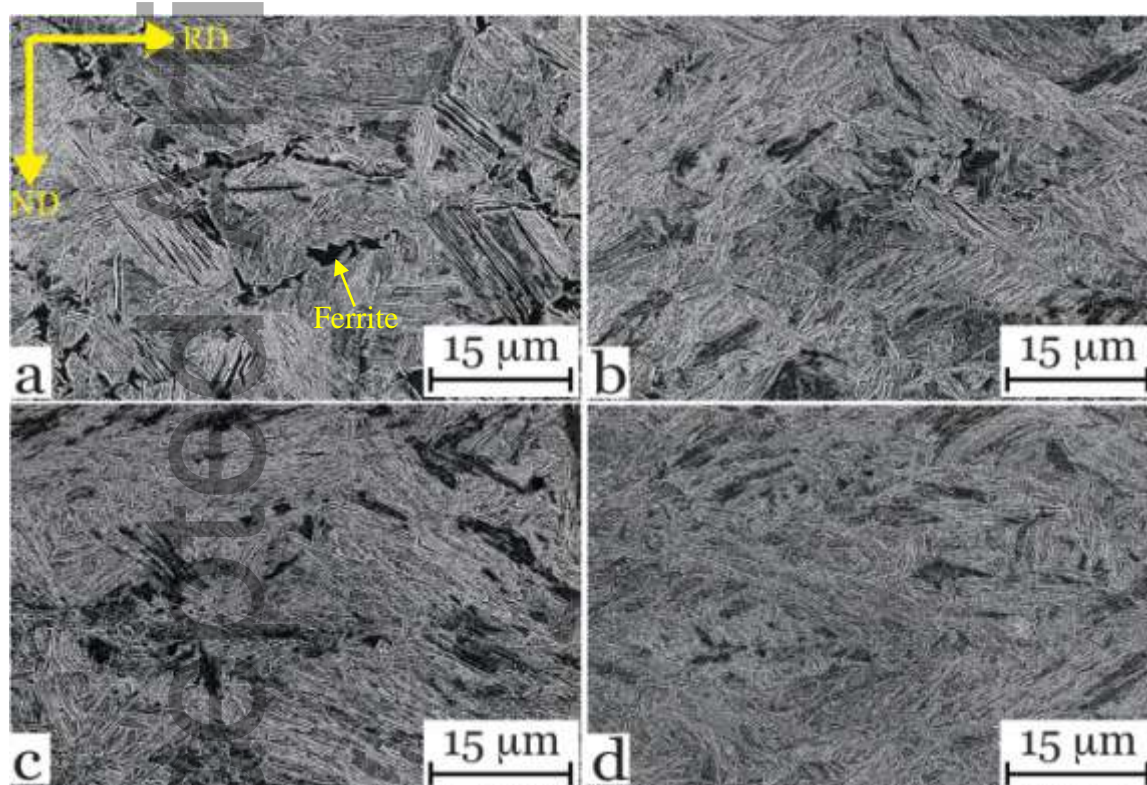
Figure 2. Typical microstructures (FESEM after etching in 2 % nital) of the investigated steels in as-quenched (DQ) condition a) 0Mo, b) 0.25Mo, c) 0.5Mo, d) 0.25Mo-Nb.

Furthermore, the microstructures in direct-quenched and tempered condition were also characterized using FESEM and those are presented in Figs. 3 and 4. Highly precipitated martensitic structures were displayed in all steels. Microstructural characterization revealed small round and needle-shape precipitates throughout all the investigated steels (Fig. 4). Generally, more and slightly smaller precipitates were noticed in Mo-Nb steels compared to other steels, as shown in Fig. 4d.
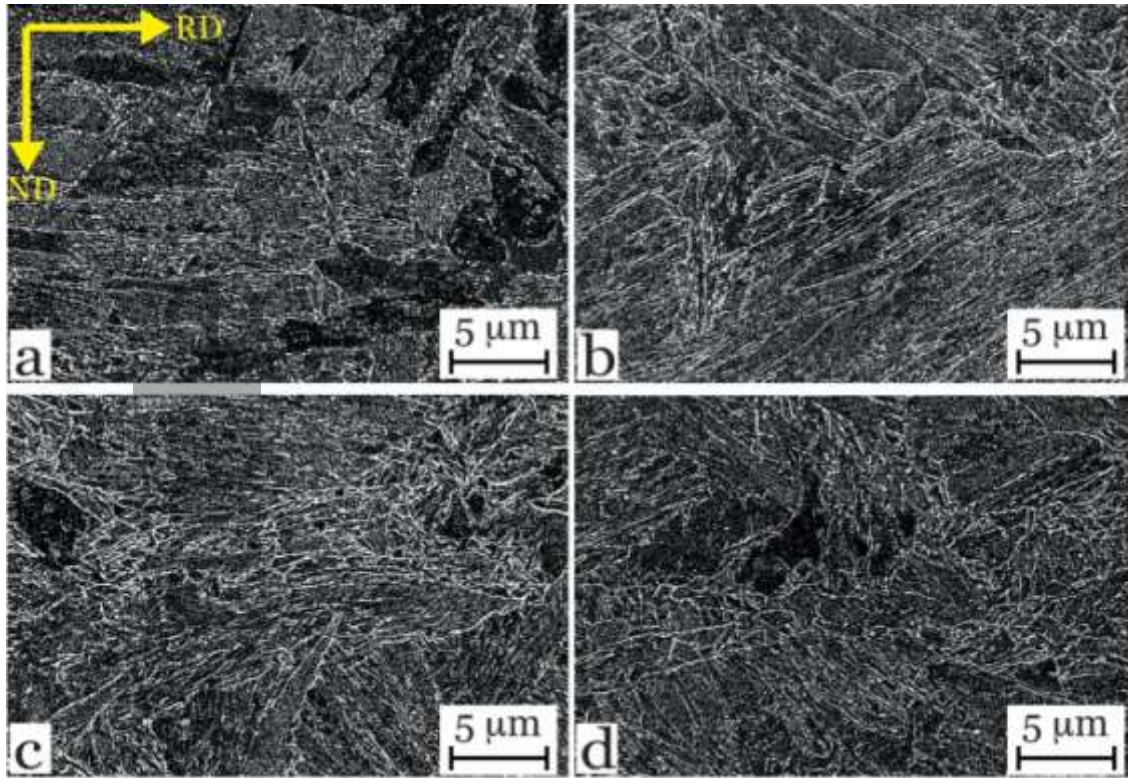
Figure 3. Typical microstructures (FESEM after etching in 2 % nital) of the investigated steels in direct-quenched and tempered (DQT) condition a) 0Mo, b) 0.25Mo, c) 0.5Mo, d) 0.25Mo-Nb.
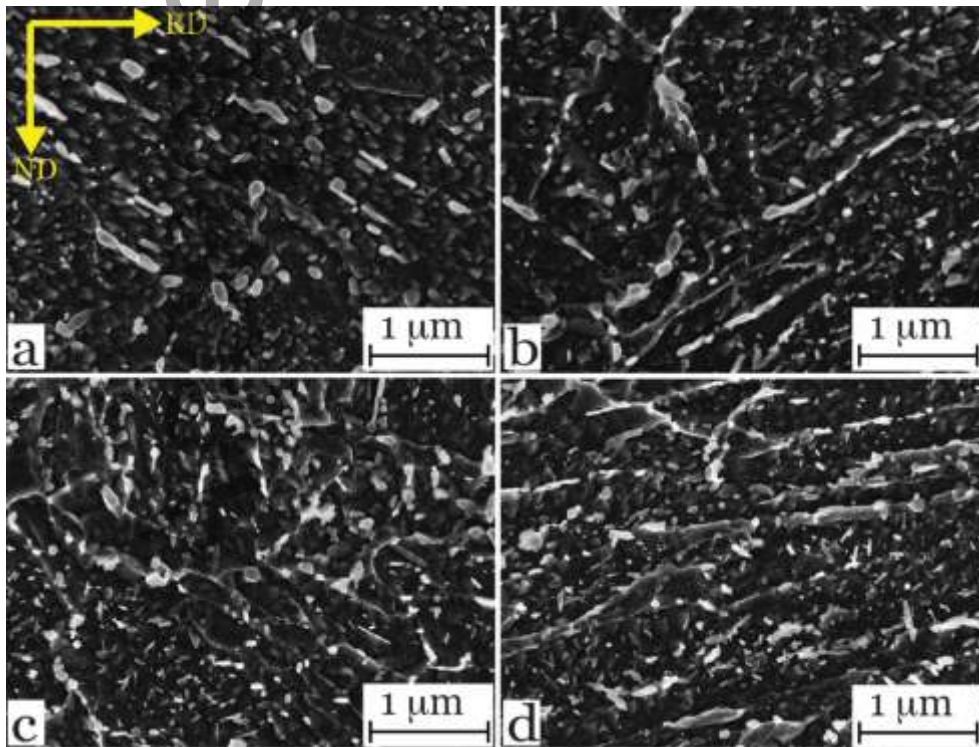

Figure 4. Carbide structure (FESEM after etching in 2 % nital) of the investigated steels in direct-quenched and tempered (DQT) condition a) 0Mo, b) 0.25Mo, c) 0.5Mo, d) 0.25Mo-Nb.

For the further characterization of small precipitates, which were not able to be identified using scanning electron microscopy, transmission electron microscopy was carried out for the investigated steels in quenched and tempered condition. Carbon extraction replicas of the samples (Fig. 5) revealed the existence of iron- and niobium carbides in the matrix. In 0Mo steel, only cementite precipitates were found with size ranging from tens to hundreds of nanometres (Fig. 5a), which can be expected, as there was no microalloying elements in this steel. In Mo-alloyed steels, no molybdenum carbides were found in replica samples. However, the iron carbide precipitates were enriched with Mo, as seen in Figs. 5b and 5c. It is known that formation of Mo_2C is driven by the enrichment of cementite as well as dissolution of cementite[19]. In the early stage of tempering, cementite particles can be assumed to contain equal amount of Mo as in the bulk of the material. As tempering proceeds, the amount of Mo in these cementite particles will increase towards the equilibrium by diffusion. In the end, cementite particles will dissolve and Mo_2C remains in the matrix. In the present study, it can be concluded that in Mo steels, the used tempering time at 600 °C (30 min at peak temperature) was not long enough to form Mo_2C precipitates in preference to cementite. Increase in Mo content from 0.25 wt.% to 0.5 wt.% produced only slightly higher concentrations of Mo in cementite particles, as seen comparing Figs. 5b and 5c. It has been shown that the dissolution of all cementite particles in Mo-alloyed steel can take up to 100 h, and maximum number density of Mo_2C precipitates are achieved after 10 h tempering at tempering temperature of 600 °C.[19]
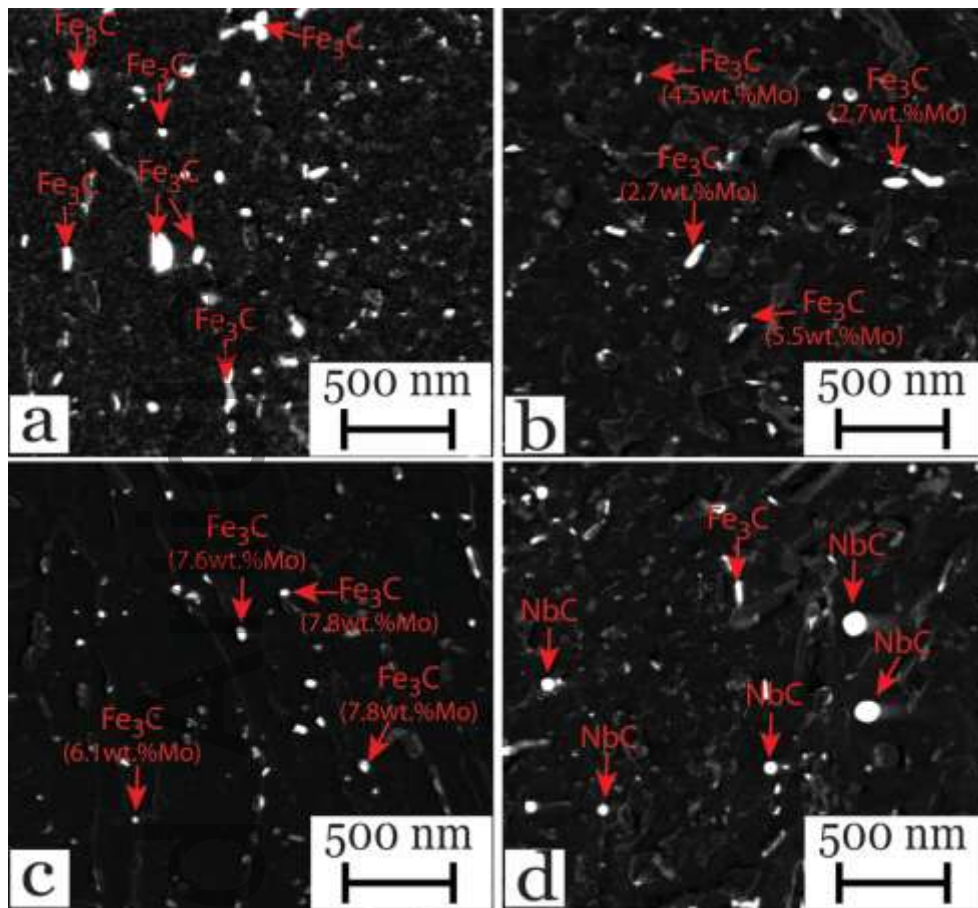
Figure 5. Carbide structure (carbon extraction replica, TEM) of investigated steels in quenched and tempered (DQT) condition a) 0Mo, b) 0.25Mo, c) 0.5Mo, d) 0.25Mo-Nb.

For further microstructure investigation, Fig. 6 presents the determined effective grain (>15 °),- lath (2-15°)- and d90% grain sizes of the investigated steels in direct quenched and direct quenched and tempered conditions based on EBSD analysis. In direct quenched condition, all steels produced similar grain sizes with no significant differences, as seen in Fig 6a. Small amount of ferrite in 0Mo steel did not have effect on the grain sizes determined using EBSD. Slight increase in all grain sizes can be seen after tempering treatment compared to DQ variants, however addition of Mo and Mo-Nb produced slightly smaller effective- and lath sizes after tempering (Fig. 6b).
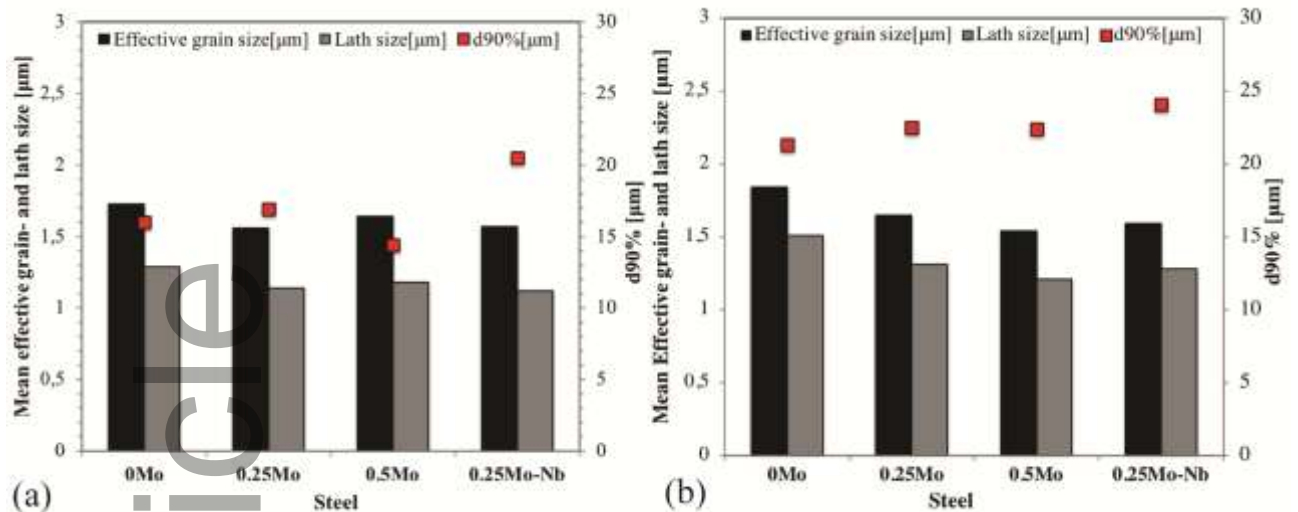
Figure 6. EBSD grain sizes of the investigated steels in a) direct quenched (DQ), b) direct quenched and tempered (DQT) conditions.

Fig. 7a shows the misorientation distributions of the direct-quenched and tempered steels and, Fig. 7b presents a comparison of the detected low-angle boundaries between DQ and DQT steels. The number of low-angle boundaries decreased significantly after tempering in case of 0Mo steel compared to other investigated steels. For 0.5Mo and Mo-Nb steels, there was no such decrease and the low-angle boundaries can be assumed to be composed of an array of dislocations. [20][21] In our study, EBSD data further verified that microalloying with Mo and Mo-Nb hindered the annihilation and movement of dislocations during the tempering process. As mentioned previously, the strongest pinning effect of dislocations was achieved with the combined alloying of Nb and Mo. Fig. 8 presents the high- and low-angle boundaries of the investigated steels with and without tempering. In case of 0Mo steel, less amount of low angle boundaries after tempering can be seen, when comparing Figs. 8a and 8e.
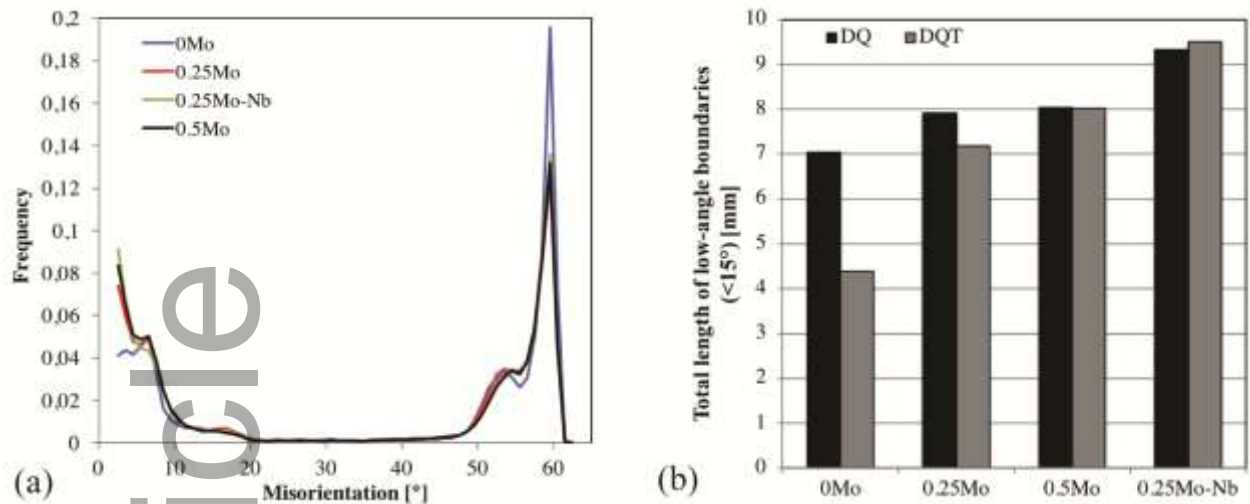
Figure 7. a) Misorientation distributions in direct-quenched and tempered condition (DQT) and b) total length of low-angle boundaries of the investigated steels.
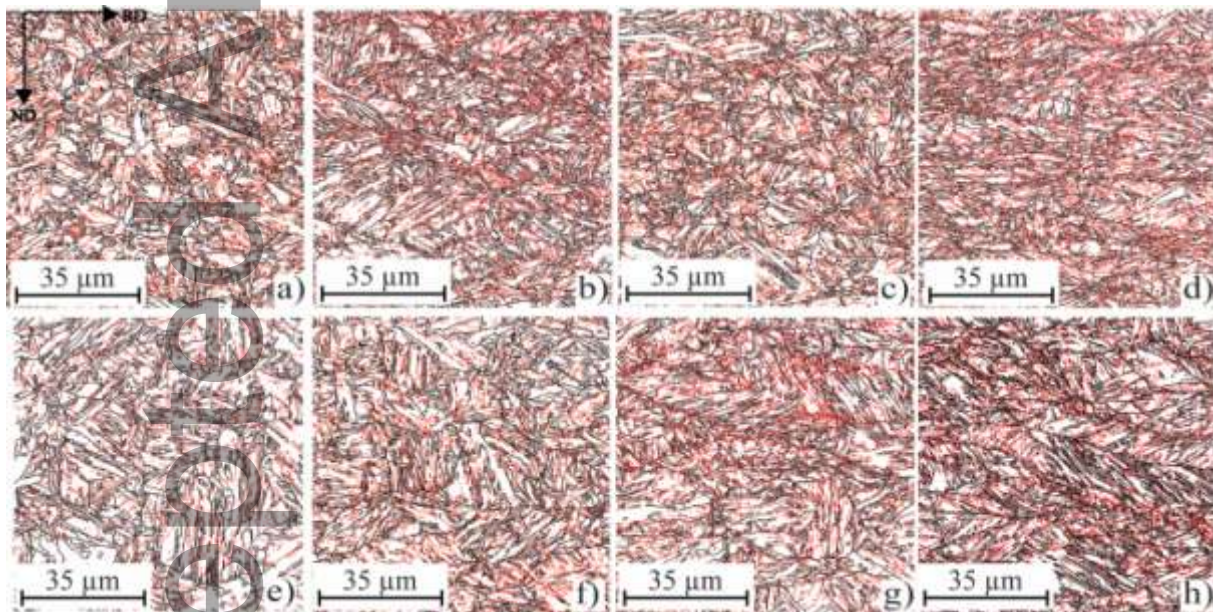

Figure 8. EBSD maps of the investigated steels showing low-angle boundaries (>2.5°, red lines) and high-angle boundaries (>15°, black lines). Upper row DQ, lower row DQT. a) & e) 0Mo, b) & f) 0.25Mo, c) & g) 0.5Mo, d) & h) 0.25Mo–Nb.

3.3. Mechanical properties after hot rolling and direct quenching

The tensile properties of the investigated steels in direct-quenched (DQ) and direct-quenched and tempered (DQT) conditions are presented in Tab. 5. The yield strength of steels in direct quenched condition were between 950 – 1119 MPa and total elongation to fracture values in range of 8.6 – 10.7 %. In as-quenched condition, the 0Mo steel showed relatively low yield and tensile strength, however the addition of 0.25 wt.% Mo enhanced the strength more than 100 MPa (Tab. 5). The lower strength of 0Mo steel can be associated with the found ferrite

formed at the prior austenite grain boundaries. Further increase in strength was achieved with higher Mo or Nb alloying, although at the expense of elongation, which moved to slightly lower values.

After tempering, generally strengthdropped, especially in respect of tensile strength, compared to as-quenched steels. However, the elongation values improved significantly after tempering. These changes in mechanical properties can be considered typical, when comparing the tempered (at high temperatures 500-650 °C) and untempered steels [22,23]. Mo and Nb alloying led to a clear increase in strength, which can be attributed to factors, such as precipitation strengthening or slowing down of the dislocation recovery due to solute drag. It has been shown that Nb tends to segregate at dislocations leading to a retardation of dislocation recovery, thus resulting in a higher density of dislocations despite treatment at high temperatures [24]. It is also known that Nb particularly forms the precipitates during subsequent heat treatment, such as tempering, leading to an increase in strength [6].

Table. 5 Tensile properties[*] of the investigated steels in direct-quenched (DQ) and direct-quenched and tempered (DQT) conditions. (0.2 % offset proof stress, tensile strength, plastic component of the uniform elongation, and total elongation to fracture with a gauge length of 5 x the specimen diameter).

FRT	Steel	$R_{p0.2}$[MPa]	R_m [MPa]	A_g [%]	A[%]	R_mxA [MPa%]
DQ	0Mo	950±10	1310±3	3.5±0.2	10.7±0.6	14661
	0.25Mo	1078±3	1436±3	3.2±0.1	10.0±0.1	15096
	0.5Mo	1119±13	1485±3	3.2±0.5	8.8±0.4	13915
	0.25Mo-Nb	1100±17	1473±7	3.3±0.1	8.6±0.5	13497
DQT	0Mo	632±2	712±2	7.5±0.2	18.3±1	13052
	0.25Mo	813±2	864±1	6.2±0.1	16.4±0.2	14157
	0.5Mo	901±2	952±2	6.1±0.1	16.1±0.5	15292
	0.25Mo-Nb	1011±2	1049±2	4.9±0.1	13.3±0.2	13951

*values average of three tests.

It can be seen that Mo addition alone was able to increase the strength after tempering compared to the non-alloyed variant (0Mo), however, the Nb alloying with combination of Mo, had the strongest effect on the strength. In fact, the 0.25Mo-Nb steel was the only steel

with over 1000 MPa yield strength after tempering treatment. Previous research [25] has elucidated the synergy effect of Mo-Nb alloying, such that Mo can reduce the activity of C and N during hot deformation leaving more solute Nb to form precipitates that can contribute to strength enhancement during tempering treatment. Comparing the R_m x A values from Table 5, the best combination of strength and tensile ductility was achieved with the 0.5Mo composition with R_m x A value of 15292 MPa%. Although, the combined alloying of Mo-Nb produced clearly highest strength value, there was a clear drop in total elongation value (13.3 %), which lower the R_m x A value (13951 MPa%) relatively much.

Impact toughness transition curves for the investigated steels with and without tempering are presented in Figs. 9a and 9b. Surprisingly, 0Mo steel had clearly the poorest impact energies in direct-quenched condition, as seen comparing transition curves in Fig 9a. Also Nb alloying produced slightly poorer impact toughness properties. The 0.25Mo steel had the best impact toughness properties after tempering with an exceptionally low 28 J transition temperature of -122 °C for the samples parallel to the rolling direction. Also, the upper shelf is reached at the low temperature of -50 °C. An addition of 0.04 wt.% of Nb to the 0.25Mo steel deteriorated impact toughness properties, and the upper shelf-energy dropped from ~135 J to ~85 J. The decrease was considered to be caused by the higher strength of the 0.25Mo-Nb steel, which could indicate that strong precipitation had occurred during tempering leading to the formation of also coarse precipitates that could contribute to lower impact toughness, thus acting as the nucleation sites for crack initiation and fracture. Many researches have shown that coarse precipitates tend to decrease the impact toughness of steels [26,27]. Previously presented TEM investigation showed that NbC precipitates existed in the matrix of Mo-Nb steel.
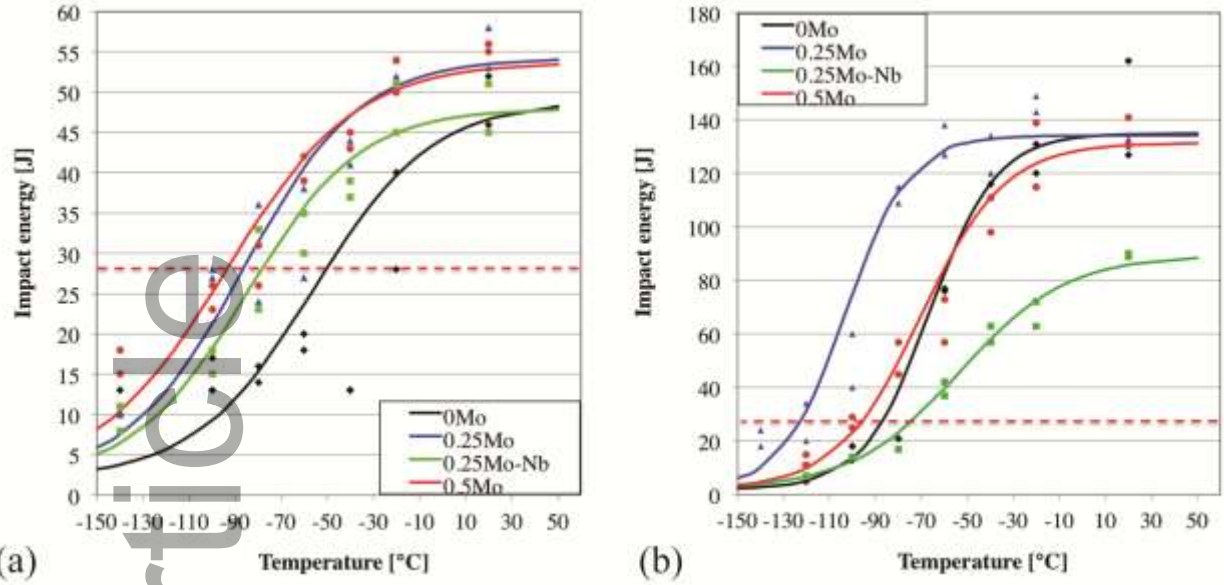
Figure 9. Transition curves based on Charpy V -notch test results in longitudinal direction, a) DQ condition, b) DQT condition.

Fig. 10 presents the comparison of yield strength and the 28 J transition temperatures of the investigated steels in the direct quenched (DQ) and direct quenched and tempered (DQT) states. The highest tempering resistance was achieved with the 0.25Mo-Nb steel, where the yield strength dropped only ~100 MPa compared to the direct-quenched variant. In the case of the two leanest compositions, 28 J transition temperatures improved after tempering, whereas for the 0.5Mo and 0.25Mo-Nb compositions, there was no significant change in transition temperature, despite the drops in yield strength (Fig. 10b.). However, 28 J transition temperatures of Mo- and Nb alloyed steels were relatively low (-73 – -113 °C) in both DQ and DQT conditions, as seen from Fig. 10b.

Fig. 11 summaries the achieved results showing the change in yield strength and 28 J transition temperatures between direct quenched and direct quenched and tempered steels. In direct-quenched condition, a significant improvement in mechanical properties was achieved with Mo and Mo-Nb alloying, as seen from Fig. 11. The Mo and Mo-Nb alloyed variants produced excellent combination of strength and toughness. In direct-quenched and tempered condition, 0.25Mo and 0.5Mo steels exhibited higher strength combined with better toughness

compared to 0Mo steel. The formed grain boundary ferrite can partially explain the relatively poor overall properties of 0Mo steel, although the amount of ferrite was relatively low, and in some parts of the sample, ferrite was not formed at all. Also, a decrease in impact toughness was noticed in the case of Nb-Mo steel after tempering especially in case of upper shelf energy, which dropped approximately 40 joules compared to other steels. This phenomenon can be related to higher strength due to precipitation hardening of NbC precipitates, as mentioned earlier. Interestingly, generally the correlation between strength and impact toughness does not follow the common perception that a higher strength produces lower impact toughness.
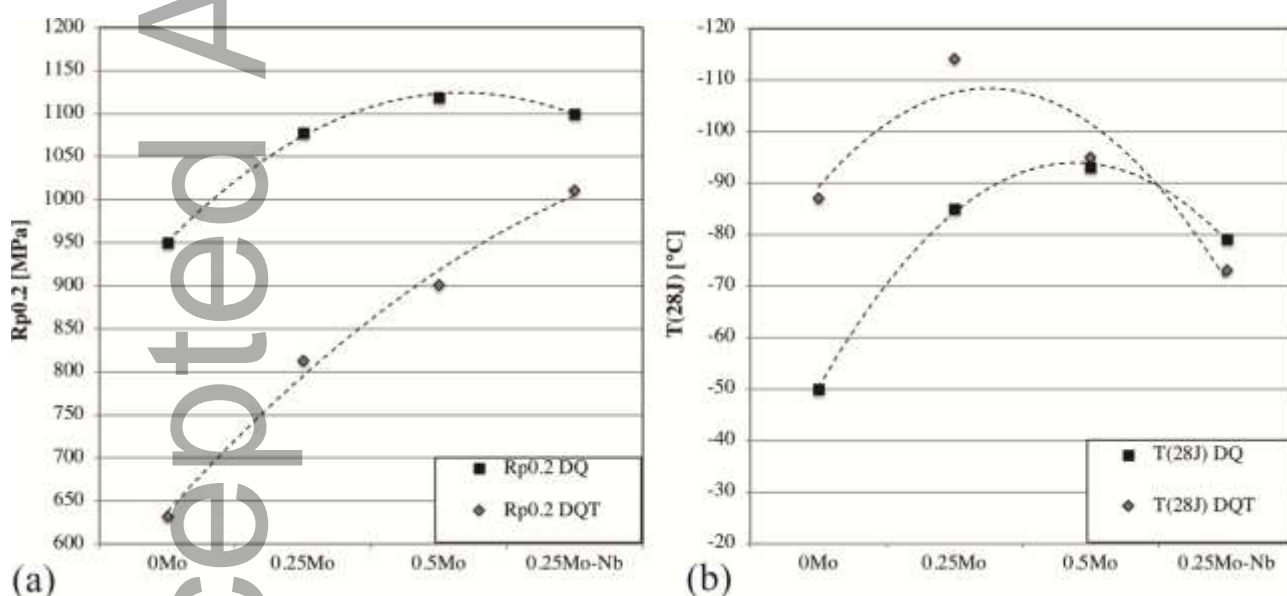

Figure. 10 a) yield strength, and b) 28J transition temperatures (longitudinal RD specimens) in both direct-quenched (DQ) and direct-tempered (DQT) conditions.
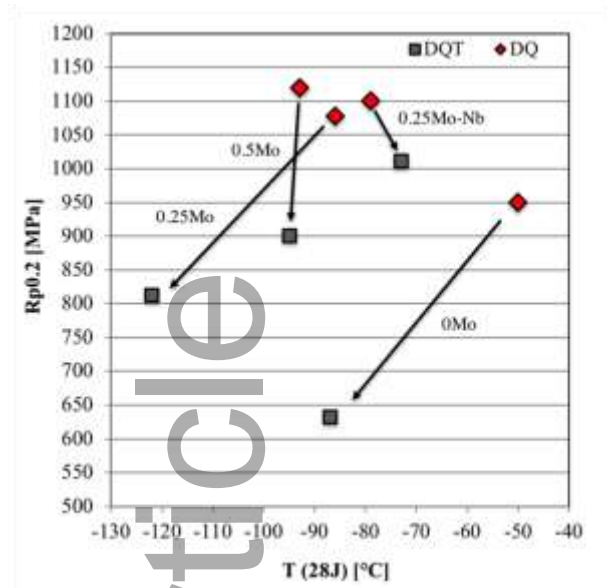
Figure. 11 Summary of yield strength and 28J transition temperatures for DQ- and DQT steels in longitudinal direction.

3.4. Correlation between mechanical properties and microstructural features

Dislocation densities of the investigated steels with and without tempering measured using XRD are presented in Fig. 12. According to the XRD measurements, the studied steels in the direct-quenched conditions produced almost equal dislocation densities giving dislocation density values of ~3 – 4 x 10^{15} m^{-2}. These values are in line with the results found in other publications. Nakashima et al. [28] reported dislocation density value of 3 x 10^{15} m^{-2} for cold rolled steel sheet, and saturation value around 10^{16} m^{-2}. Also Morito et al. [29] showed similar dislocation density values of ~1 – 4 x 10^{15} m^{-2} for martensitic steels. Slight differences can be noticed by comparing the dislocation densities of the direct-quenched samples, although no statistically acceptable conclusions can be made. As expected, tempering reduced the dislocation densities producing dislocation density values of 2.8 x 10^{14} – 1.3 x 10^{15} m^{-2}, as seen from Fig. 12. However, it can be seen that Mo and Mo-Nb alloying clearly hindered the decrease of dislocation densities during tempering. The most significant effect can be achieved by Mo-Nb alloying. As mentioned earlier, solutes Nb and Mo can create strong solute drag effect, and also NbC precipitates can create strong pinning effect on dislocations [24][30][31]. Based on the TEM observations shown previously (Fig. 5), the role of Mo on

preserving the high dislocation density was based on solute drag effect, and in the case of 0.25Mo-Nb steel, also the effect of NbC precipitates in strongly pinning the dislocations led to even higher dislocation density after tempering.

Fig. 12b presents the correlation between measured dislocation densities and yield strength ($R_{p0.2}$) of direct quenched and tempered samples. A high correlation can be noticed between the measured values. However, it must be emphasized that though the dislocation density affects the yield strength, it cannot be determined just by estimating the dislocation density of the martensitic steel.
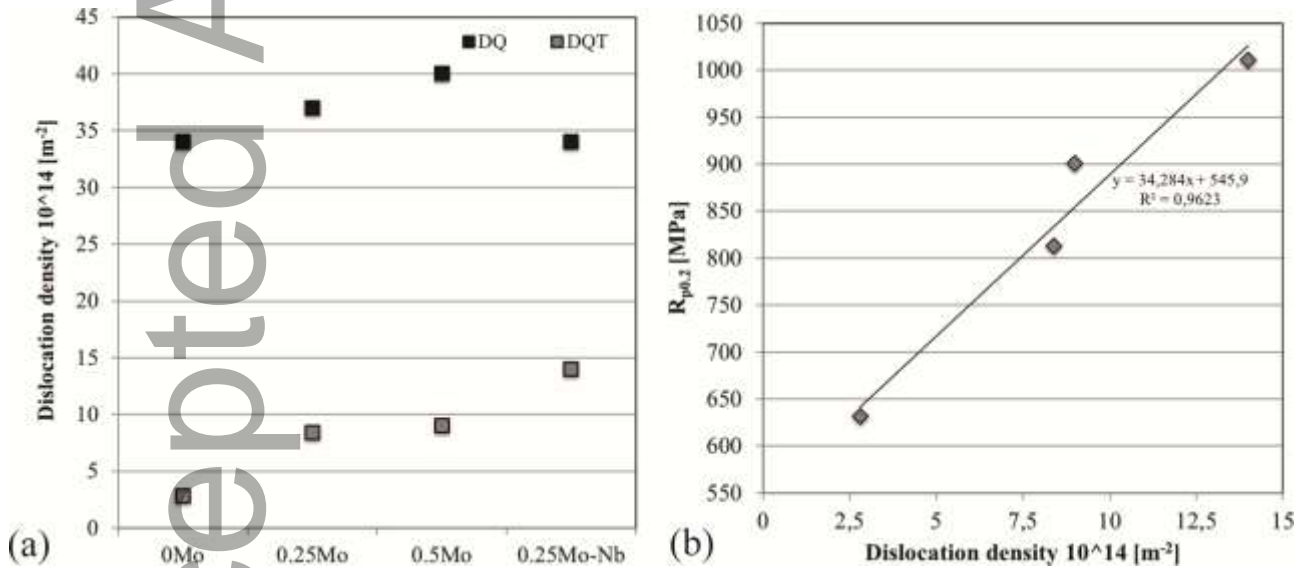

Figure 12. a) Dislocation densities of the investigated steels, b) correlation of yield strength and dislocation densities of direct quenched and tempered (DQT) steels.

According to Young and Bhadeshia [32] the strength of bainite and martensite can be factorized as follows in Equation 4:

$$\sigma = \sigma_{Fe} + \sum_i \sigma_{SS}^i + \sigma_C + k_\epsilon (\bar{L}_3)^{-1} + \sigma_{ppt} + K_D \rho_d^{0.5} \tag{4}$$

where σ_{Fe} is strengthening contribution of pure bcc iron in a fully annealed condition (150 MPa [33]), σ_{ss}^i is solid solution strengthening due to substitutional solute i, σ_C is solid solution strengthening due to carbon, σ_{ppt} is precipitation strengthening from carbide particles and k_ϵ $(\bar{L}_3)^{-1}$ is the lath size strengthening component including the constant k_ϵ, which for martensite

is reported to be 115 MPa m and $\overline{L}_3$ is mean linear intercept of laths measured at random orientations on random sections [32]. $K_D\rho_d^{0.5}$ represents the dislocation strengthening component of the model, where the ρ is dislocation density, constant K_D is 0.38μb for bcc metals, μ is the shear modulus (here taken as 82 GPa for Fe) and b is the burgers vector (0.2485 nm in the present case[34]).

Based on equation 4 and the term $K_D\rho_d^{0.5}$,which corresponds to the effect of dislocation density in strengthening, the calculated strengthening factor for dislocation density in DQ and DQT samples are presented in Fig. 13. As seen from the values given in Fig. 13, the difference in dislocation density values between DQ steels did not have any effect on the strengthening of martensite. However, in DQT steels, clearly the higher dislocation density values of Mo and Mo-Nb alloyed steels have effect on the strength of DQT steels. The difference in measured strengthof 0Mo steel in DQ and DQT conditions corresponds well with the difference in calculated strengthening factors presented in Fig. 13. However, it must be noticed that not only dislocation density affects the strengthening of the tempered steels especially in case of microalloyed steels. Precipitation strengthening has large effect also, which can be seen especially in Mo-Nb steel, where yield strength dropped less than 100 MPa after tempering compared to direct quenched variant implying that the difference in yield strength was considerably lower than the predicted values given in Fig. 13 (436 MPa vs. 266 MPa).
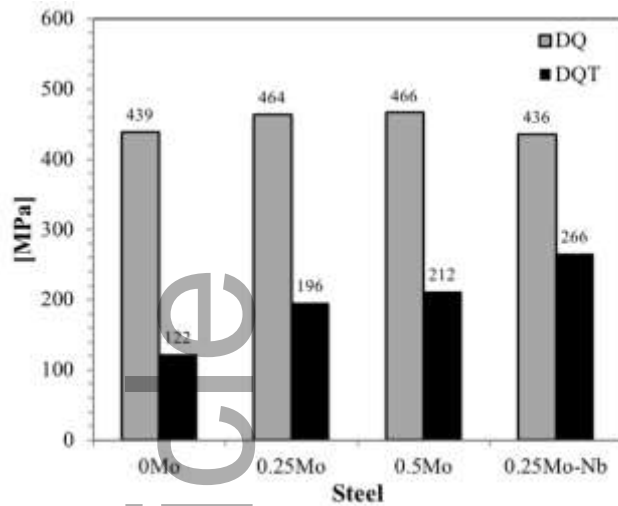
Figure 13. Effect of dislocation density on strengthening of the investigated steels.

4. Summary and conclusions

The effect of molybdenum and niobium on the microstructures and mechanical properties of laboratory rolled and direct-quenched and direct-quenched and tempered steel plates containing 0.16 wt.% C has been studied. A finish rolling temperature of 900 °C was used for these TMCP trials. The plates were direct-quenched to room temperature using a cooling rate in range of 40-50 °C/s. Tempering was executed on selected hot rolled samples using a peak temperature of 600 °C and a 30 minutes of holding time. Based on the results, the following conclusions can be drawn:

Mo and Nb microalloying raise the T_{NR} temperature leading to a more pancaked austenite structure and higher S_v values, leading to a greater refinement and randomization. There is a strong synergy between Nb and Mo.

Based on FESEM-EBSD analysis, microstructures were fully martensitic in as-quenched condition, except the 0Mo steel had small amount of ferrite. However, there were no significant differences in the lath sizes, mean effective grain sizes, or the 90th percentile effective grain sizes among the different compositions studied. Also, misorientation distributions were identical and typical formartensitic microstructures. In quenched and tempered condition, no molybdenum carbides were noticed, except the cementite particles

saturated with Mo content. NbC precipitates were found in Mo-Nb steel and no molybdenum carbides were seen in the replicas.

Mo and Mo-Nb microalloying increases the strength and improves impact toughness of the steels in direct-quenched state compared to the non-alloyed version. Remarkably good combination of strength and toughness was achieved especially in Mo-alloyed variants in direct-quenched conditions. A marginal drop increase in impact transition temperature (T28J) arose in the case of Nb-Mo steel presumably due to the presence of an inhomogeneous prior austenite structure.

Mo and Nb additions increased strengthsignificantly in the direct-quenched and tempered state owing to higher dislocation densities and copious precipitation hardening. 0.25Mo-Nb steel was the only steel with over 1000 MPa yield strength after tempering. Presumably, this was due to molybdenum reducing the activity of carbon and nitrogen, allowing niobium in solution to form precipitates during tempering rather than precipitation during hot rolling. However, Nb microalloying decreased the impact toughness due to an intense precipitation hardening. 0.25Mo steel had the best 28 J transition temperature properties (-120 °C) in the tempered condition. Effect of molybdenum on tempering resistance was related to solute drag leading to higher dislocation density. No molybdenum carbides were discovered in the microstructure of DQT steels.

XRD analysis showed that the addition of Mo and Mo-Nb alloying reduced the annihilation and rearrangement of dislocations during tempering, which, together with precipitation hardening, led to higher strength. EBSD analysis showed similar results indicating that high dislocation density after tempering can be achieved by Mo and Mo-Nb alloying.

References

1. Hawk, J.; Wilson, R. Tribology of Earthmoving, Mining, and Minerals Processing. In *Modern Tribology Handbook: Volume One: Principles of Tribology*; 2000; pp. 1331–1370 ISBN 9780849377877.

2. Ratia, V.; Valtonen, K.; Kemppainen, A.; Kuokkala, V.-T. High-Stress Abrasion and Impact-Abrasion Testing of Wear Resistant Steels. *Tribol. Online***2013**, *8*, 152–161.

3. Krauss, G. Heat-Treated Low-Alloy Carbon Steels: The Benefits of Molybdenum. *Int. Semin. Appl. Mo Steels June 27th - 28th***2010**, 14–24.

4. OGINO, Y.; TANIDA, H.; KITAURA, M.; ADACHI, A. Effect of Niobium Addition on Austenite Grain Size in Steels. *Tetsu-to-Hagane***1971**, *57*, 533–546.

5. Hannula, J.; Porter, D.; Kaijalainen, A.; Somani, M.; Kömi, J. Mechanical Properties of Direct-Quenched Ultra-High-Strength Steel Alloyed with Molybdenum and Niobium. *Metals (Basel).***2019**, *9*, 350.

6. Xie, Z.J.; Ma, X.P.; Shang, C.J.; Wang, X.M.; Subramanian, S.V. Nano-sized precipitation and properties of a low carbon niobium micro-alloyed bainitic steel. *Mater. Sci. Eng. A***2015**, *641*, 37–44.

7. Wang, Z.; Zhu, X.; Liu, W. Influence of Mo on tempering precipitation in Nb-Mo-V microalloyed steels. *Chinese J. Mater. Res.***2010**, *24*, 217–222.

8. Chen, Y.-W.; Huang, B.-M.; Tsai, Y.-T.; Tsai, S.-P.; Chen, C.-Y.; Yang, J.-R. Microstructural evolutions of low carbon Nb/Mo-containing bainitic steels during high-temperature tempering. *Mater. Charact.***2017**, *131*, 298–305.

9. Saastamoinen, A.; Kaijalainen, A.; Porter, D.; Suikkanen, P.; Yang, J.-R.; Tsai, Y.-T. The effect of finish rolling temperature and tempering on the microstructure, mechanical properties and dislocation density of direct-quenched steel. *Mater. Charact.***2018**, *139*, 1–10.

10. Huang, B.M.; Yang, J.R.; Yen, H.W.; Hsu, C.H.; Huang, C.Y.; Mohrbacher, H. Secondary hardened bainite. *Mater. Sci. Technol.***2014**, *30*, 1014–1023.

11.   Metallic materials - Tensile testing - Part 1: Method of test at room temperature. *ISO 6892-12016***2016**.

12.   Metallic materials - Charpy pendulum impact test - Part 1: Test method. *ISO 148-12016***2016**.

13.   Brownrigg, A.; Curcio, P.; Boelen, R. Etching of prior austenite grain boundaries in martensite. *Metallography***1975**.

14.   Higginson, R.L.; Sellars, C.M. *Worked Examples in Quantitative Metallography*; Maney: London, 2003; ISBN 1902653807.

15.   Williamson, G.K.; Hall, W.H. X-Ray broadening from filed aluminium and tungsten. *Acta Metall.***1953**, *1*, 22–31.

16.   Williamson, G.K.; Smallman, R.E. III. Dislocation densities in some annealed and cold-worked metals from measurements on the X-ray debye-scherrer spectrum. *Philos. Mag.***1956**, *1*, 34–46.

17.   Pereda, B.; Fernández, A.I.; López, B.; Rodriguez-Ibabe, J.M. Effect of Mo on Dynamic Recrystallization Behavior of Nb-Mo Microalloyed Steels. *ISIJ Int.***2007**, *47*, 860–868.

18.   Schambron, T.; Dehghan-Manshadi, A.; Chen, L.; Gooch, T.; Killmore, C.; Pereloma, E. Effect of Mo on dynamic recrystallization and microstructure development of microalloyed steels. *Met. Mater. Int.***2017**, *23*, 778–787.

19.   Yamasaki, S.; Bhadeshia, H.K.D.H. Modelling and characterisation of Mo 2 C precipitation and cementite dissolution during tempering of Fe–C–Mo martensitic steel. *Mater. Sci. Technol.***2003**, *19*, 723–731.

20.   Guleryuz, E.; Mesarovic, S. Dislocation Nucleation on Grain Boundaries: Low Angle Twist and Asymmetric Tilt Boundaries. *Crystals***2016**, *6*, 77.

21.   Tochigi, E.; Nakamura, A.; Shibata, N.; Ikuhara, Y. Dislocation Structures in Low-Angle Grain Boundaries of α-Al2O3. *Crystals***2018**, *8*, 133.

22.   Saastamoinen, A.; Kaijalainen, A.; Heikkala, J.; Porter, D.; Suikkanen, P. The effect of tempering temperature on microstructure, mechanical properties and bendability of direct-quenched low-alloy strip steel. *Mater. Sci. Eng. A***2018**, *730*, 284–294.

23.   Dhua, S.K.; Ray, A.; Sarma, D.S. Effect of tempering temperatures on the mechanical properties and microstructures of HSLA-100 type copper-bearing steels. *Mater. Sci. Eng. A***2001**, *318*, 197–210.

24.   Takahashi, J.; Kawakami, K.; Hamada, J.; Kimura, K. Direct observation of niobium segregation to dislocations in steel. *Acta Mater.***2016**, *107*, 415–422.

25. Akben, M.G.; Weiss, I.; Jonas, J.J. Dynamic precipitation and solute hardening in A V microalloyed steel and two Nb steels containing high levels of Mn. *Acta Metall.***1981**, *29*, 111–121.

26. Bepari, M.M.A. Effects of precipitates on strength and toughness of vanadium structural steels. *Mater. Sci. Technol.***1990**, *6*, 338–348.

27. Zheng, Y.; Wang, F.; Li, C.; Li, Y.; Cheng, J.; Cao, R. Effect of Microstructure and Precipitates on Mechanical Properties of Cr–Mo–V Alloy Steel with Different Austenitizing Temperatures. *ISIJ Int.***2018**, *58*, 1126–1135.

28. Nakashima, K.; Suzuki, M.; Futamura, Y.; Tsuchiyama, T.; Takaki, S. Limit of Dislocation Density and Dislocation Strengthening in Iron. *Mater. Sci. Forum***2006**, *503–504*, 627–632.

29. Morito, S.; Nishikawa, J.; Maki, T. Dislocation Density within Lath Martensite in Fe–C and Fe–Ni Alloys. *ISIJ Int.***2003**, *43*, 1475–1477.

30. Weiss, I.; Jonas, J.J. Interaction between recrystallization and precipitation during the high temperature deformation of HSLA steels. *Metall. Trans. A***1979**, *10*, 831–840.

31. Shrestha, S.L.; Xie, K.Y.; Ringer, S.P.; Carpenter, K.R.; Smith, D.R.; Killmore, C.R.; Cairney, J.M. The effect of clustering on the mobility of dislocations during aging in Nb-microalloyed strip cast steels: In situ heating TEM observations. *Scr. Mater.***2013**, *69*, 481–484.

32. Bhadeshia, H.K.D.H.; Young, C.H. Strength of mixtures of bainite and martensite. *Mater. Sci. Technol.* 1994, *10*, 209–214.

33. Hutchinson, B.; Hagström, J.; Karlsson, O.; Lindell, D.; Tornberg, M.; Lindberg, F.; Thuvander, M. Microstructures and hardness of as-quenched martensites (0.1–0.5%C). *Acta Mater.***2011**, *59*, 5845–5858.

34. Bouaziz, O.; Lung, T.; Kandel, M.; Lecomte, C. Physical modelling of microstructure and mechanical properties of dual-phase steel. In Proceedings of the Journal De Physique. IV : JP; 2001.

Evaluation of Mechanical Properties and microstructures of Direct-Quenched- and direct quenched and tempered Microalloyed Ultrahigh-Strength Steels

Short summary:

The present investigation showed that Mo prevents softening during tempering mainly by effective solute drag leading to high dislocation densities. Addition of Nb combines strong precipitation strengthening and solute drag leading to even higher hardness after tempering at the expense of slightly deteriorated impact toughness. However, superior mechanical properties can be achieved with Mo and Mo-Nb alloying both in DQ- and DQT conditions.

Image for theTable of Contents: